NUMERICAL MODELING OF TWO-DIMENSIONAL ADVECTION-DISPERSION IN OPEN CHANNEL

Myung Eun Lee [1], Young Han Kim [2] and Il Won Seo [3]

[1] Graduate Student, Dept. of Civil Engineering, Seoul National University, Seoul, Korea
[2] Post Doctor, Dept. of Civil Engineering, Seoul National University, Seoul, Korea
[3] Professor, Dept. of Civil Engineering, Seoul National University, Seoul, Korea

Abstract: Two-dimensional depth–averaged advection-dispersion equation was simulated using FEM. In the straight rectangular channel, the advection-dispersion processes are simulated so that these results can be compared with analytical solutions for the transverse line injection and the point injection. In the straight domain the standard Galerkin method with the linear basis function is found to be inadequate to the advection-dispersion analysis compared to the upwind finite element scheme. The experimental data in the S-curved channel were compared with the result by the numerical model using SUPG(Streamline upwind Petrov-Galerkin) method.

Keywords: advection-dispersion equation, meandering channel, experiments, Galerkin method, upwind FEM, SUPG method

1. INTRODUCTION

The traditional one-dimensional advection-dispersion model is not applicable until the end of an initial period, which is the time required for the cross-sectional concentration distribution to become nearly uniform and independent of the geometrical configuration of the source. The initial period restriction can be a serious problem for wide rivers since the length of the initial period may be the same order as the length of the entire reach under consideration (Basha, 1997). So, it will be necessary to use a multi-dimensional model when the initial mixing is considered to be important.

A three-dimensional model will be adequate to simulate the complicate river mixing accurately but it requires considerable time and cost which make the model inefficient. Moreover, particularly in natural river, the scale of depth is almost negligible compared to the magnitude of river width, so the vertical mixing is completed much faster than the transverse mixing. Thus, in this study, the two-dimensional model is chosen to investigate the longitudinal and transverse mixing in the open channel.

The numerical modeling for the two- dimensional advection-dispersion equation has been attempted by the finite difference approximation. Motivated by the fact that the propagation of

information is in the direction of flow velocity, the finite difference practitioners Runchell et al.(1969), Spalding(1972), and Barrett(1974) were the first to overcome the approximation problem using various formulae which combine central and backward differences. However the finite difference method has a limitation in grid generation for the complex meandering channel commonly encountered in natural river. This configuration problem may be treated more effectively by the finite element method.

The general finite element scheme that has been applied to the common partial differential equations is called Galerkin method. The Galerkin method, when applied to most structures and heat conduction problems, leads to symmetric stiffness matrices and by these matrices the solution possesses the 'best-approximation' property (Brooks & Hughes, 1982). However, in the advection problem the matrix related to the advection term is non-symmetric so that the 'best-approximation' property cannot be retained. In practice, these shortcomings appear as a wiggling solution in the advection dominated condition which forces a rapid change in the solution near the boundary.

The necessity for upwind finite element scheme is due to this wiggling solution produced when the advection is dominant. The basic idea of the upwind method is to use the alternative weighting function different to the shape function and that is the only difference between this method and the common Galerkin method. Such weighting functions were first suggested by Zienkiewicz *et al.* (1976) and actually used by Christie *et al.* (1976).

Heinrich *et al.* (1977) used the parabolic upwind weighting functions in steady-state one dimensional problem and proposed the extension of this weighting to the two-dimensional conditions of crosswind were not considered. In the multi-dimensional problem, there is unintended numerical dispersion normal to the streamline direction by this approach because of the false numerical dispersion inherent in the upwinding. So it is necessary to modify the upwind scheme to match the multi-dimensional problem. The streamline upwind Petrov-Galerkin (SUPG) method which introduce the additional diffusion only along the streamline was developed by this motivation. By this method, in two (or three) dimensions the advection is only active in the direction of the resultant element velocity. Han and Kim (2000) developed Petrov-Galerkin finite element method for hydrodynamic and advection-diffusion analysis in a river. And Kim and Han (2000) applied the Petrov-Galerkin finite element model to the hydrodynamics and water quality control problem of the main Nakdong River from Sengju to Hyunpoong.

There is commercial software RMA4 which is the contamination transport model of the SMS (Surface Modeling System) and this used for the model verification in this study. RMA4 uses the fluid dynamic solutions of RMA2 to define the velocity field of the given mesh. RMA2 was developed by Norton, King, Orlob (1973) of Water Resources Engineers, for the Walla Walla District, Corps of Engineers. Subsequent enhancement was done by King and Norton, of Resources Management Associates (RMA) and Waterways Experiment Station Hydraulics Laboratory, US Army Corps of Engineers (USACE-WES). These model such as RMA2 and RMA4 and other water analysis models constitute SMS which provide various post process operation with calculated results. Kim *et al.* (1998) used this RMA model to predict the contaminant transport in the region of Han River from downstream of Cham-Sil weir to upstream of Shin-Kok weir. RMA models used Galerkin

method in their formulation, so their will be the possibility of improvement by current study of advection transport formulation using finite element method.

The main objective of this research is to formulate the numerical algorithm by the finite element method in order to analyze two-dimensional mixing in the meandering channel. The SUPG scheme was employed for the numerical formulation. The experimental results of mixing in the S-curved channel are compared with the numerical results to test the applicability of the proposed model.

2. MATHEMATICAL MODEL

2.1 Governing Equation

The correct procedure for depth averaging the three-dimensional advection-diffusion equation is to integrate each term over the depth taking careful account of any depth variations of velocity and concentration. We begin this procedure from a three-dimensional advection- diffusion equation in Cartesian coordinates.

$$\frac{\partial \bar{c}}{\partial t}+\frac{\partial}{\partial x}(\bar{u}_x\bar{c})+\frac{\partial}{\partial y}(\bar{u}_y\bar{c})+\frac{\partial}{\partial z}(\bar{u}_z\bar{c}) = \frac{\partial}{\partial x}\left(e_x\frac{\partial \bar{c}}{\partial x}\right)+\frac{\partial}{\partial y}\left(e_y\frac{\partial \bar{c}}{\partial y}\right)+\frac{\partial}{\partial z}\left(e_z\frac{\partial \bar{c}}{\partial z}\right) \quad (1)$$

where $\bar{c}$ is the time-averaged concentration, $\bar{u}_x, \bar{u}_y$ and $\bar{u}_z$ are the each directional time-averaged velocities, and e_x, e_y and e_z denote the directional turbulent diffusion coefficients for corresponding directions.

The depth averaged form of this equation can be derived by integrating Eqn. (1) from the bed to the water surface using Leibnitz's rule. Then using the Reynolds' decomposition and Taylor's analysis of turbulent shear flow, the following simplified depth averaged equation can be derived readily.

$$\frac{\partial C}{\partial t}+\frac{\partial}{\partial x}(d_cUC)+\frac{\partial}{\partial y}(d_cVC) = \frac{\partial}{\partial x}\left[d_c(e_x+D_x)\frac{\partial C}{\partial x}\right]+\frac{\partial}{\partial y}\left[d_c(e_y+D_y)\frac{\partial C}{\partial y}\right] \quad (2)$$

where D_x and D_y are the longitudinal and transverse dispersion coefficients which account for the effects on the depth-averaged tracer concentration of depth variations in the longitudinal velocity, and d_c represents local depth of the channel. C denotes the depth averaged value of the tracer concentration, and U and V directional velocities in x and y directions, respectively.

$$C=\frac{1}{d_c}\int \bar{c}dy,\quad U=\frac{1}{d_c}\int \bar{u}_x dy,\quad V=\frac{1}{d_c}\int \bar{u}_y dy$$

Invariably in river channels $D_x >> e_x$ and $D_y >> e_y$. Using the continuity equation, Eqn. (2) can be rewritten in advection form as follows.

$$\frac{\partial C}{\partial t}+U\frac{\partial C}{\partial x}+V\frac{\partial C}{\partial y} = \frac{1}{d_c}\frac{\partial}{\partial x}\left[d_cD_x\frac{\partial C}{\partial x}\right]+\frac{1}{d_c}\frac{\partial}{\partial y}\left[d_cD_y\frac{\partial C}{\partial y}\right] \quad (3)$$

2.2 Numerical Modeling

When the channel depth and dispersion coefficient are assumed to have constant values to simplify the problem and the variable of channel depth is eliminated using constant depth condition, Eqn. (3) becomes

$$\frac{\partial C}{\partial t}+U\frac{\partial C}{\partial x}+V\frac{\partial C}{\partial y}-D_x\frac{\partial^2 C}{\partial x^2}-D_y\frac{\partial^2 C}{\partial y^2}=0 \quad (4)$$

When the approximated value of the concentration is expressed as $\hat{C}$, residuals of Eqn. (4) is

$$R=\frac{\partial \hat{C}}{\partial t}+U\frac{\partial \hat{C}}{\partial x}+V\frac{\partial \hat{C}}{\partial y}-D_x\frac{\partial^2 \hat{C}}{\partial x^2}-D_y\frac{\partial^2 \hat{C}}{\partial y^2} \quad (5)$$

The weighted residual formulation in the finite element method is

$$\int_{\Omega^e} R\cdot w_i d\Omega^e = 0, \quad i=1,2,...,N \quad (6)$$

where w_i is a weighting function for each i-th segment of finite elements.

Above integration with respect to the whole domain produces the following matrix equation

$$[M_{ij}]\dot{\vec{\hat{C}}}_t+([U_{ij}]+[K_{ij}])\vec{\hat{C}}=0 \quad (7)$$

where

$$M_{ij}=\int_{\Omega^e} w_i N_j d\Omega^e$$

$$U_{ij}=\int_{\Omega^e} w_i\left[U\frac{\partial N_j}{\partial x}+V\frac{\partial N_j}{\partial y}\right]d\Omega^e$$

$$K_{ij}=\int_{\Omega^e}\left[D_x\frac{\partial w_i}{\partial x}\frac{\partial N_j}{\partial x}+D_y\frac{\partial w_i}{\partial y}\frac{\partial N_j}{\partial y}\right]d\Omega^e$$

About $\dot{\vec{\hat{C}}}_t$ we take the finite difference approximation for appropriate time step Δt.

$$\hat{C}_t\approx\frac{\hat{C}^{n+1}-\hat{C}^n}{\Delta t} \quad (8)$$

The SUPG method introduced by Brooks and Hughes (1982) can be readily accomplished by taking the individual weighting function for each node i as

$$w_i=N_i+\frac{\alpha h}{2}\frac{U(\partial N_i/\partial x)+V(\partial N_i/\partial y)}{|\vec{U}|} \quad (9)$$

where optimal α is determined for each element as

$$\alpha_{opt}=\coth|Pe|-\frac{1}{|Pe|} \quad (10)$$

with local Peclet number $Pe=|\vec{U}|h/(2k)$ where h is the maximum size of the element in the direction of the velocity vector and k is the diffusion coefficient. The form of Eqn. (9) is such that the 'non-standard' weighting has a zero effect in the direction in which the velocity component is zero. Thus the balancing diffusion is only introduced in the direction of the resultant velocity vector $\vec{U}$ (Zienkiewicz and Taylor, 2000).

Integration of the derivatives with the local coordinate system no longer involves simple polynomial due to the term $1/|J|$ appearing in the inverse Jacobian matrix and become troublesome. For this, the procedure known as Gaussian quadrature was used which is the most common numerical integration to solve this difficulty.

With respect to the term of $\hat{C}$, we can express this as the combination of the values of each time step.

$$\hat{C}=\theta\hat{C}^{n+1}+(1-\theta)\hat{C}^n \quad (11)$$

Setting θ as 1/2, the final matrix equation will become a Crank-Nicolson approximation.

$$[M_{ij}]\frac{\vec{\hat{C}}^{n+1}-\vec{\hat{C}}^n}{\Delta t}+([U_{ij}]+[K_{ij}])\frac{\vec{\hat{C}}^{n+1}+\vec{\hat{C}}^n}{2}=0 \quad (12)$$

3. MODEL VERIFICATION

3.1 Line Source

To test the applicability of the finite element

model, the transverse line source problem with steady injection in the constant depth straight rectangular channel was solved. This simple case can be compared with the one-dimensional analytical solution of continuous injection problem. The analytical solution for this one-dimensional problem is given as

$$C = \frac{C_o}{2}\left[erfc\left(\frac{x-Ut}{\sqrt{4D_x t}}\right) + \exp\left(\frac{Ux}{D_x}\right) erfc\left(\frac{x+Ut}{\sqrt{4D_x t}}\right)\right] \tag{13}$$

Both the standard Galerkin method and the Petrov-Galerkin method used for this comparison. Fig. (1) shows the comparing result at $t = 36$, 73, 108 sec. In this simulation, $U = 0.5\ m/s$, $\Delta x = 2.5\ m$, $\Delta y = 2\ m$, $\Delta t = 3.6$ sec, and D_x varies with Peclet number. As time goes by, the numerical solution by standard Galerkin method shows a wiggling one as the Peclet number is increased, as shown in Fig. (1b). This result shows that the standard Galerkin method is not only inappropriate for steady-state problems, which is well-known, but also for the transient problems.

3.2 Point Source

In the line source injection problem, the solutions by Petrov-Galerkin method well-matched with the analytical solutions. Then it is necessary to test the model by the Petrov-Galerkin method whether it is applicable to the two- dimensional motion of mixing process. The point source problem is tested also in the same straight channel and then compared with the analytical solution. The analytical solution for this point source problem accounting boundary effects from the both sides of the channel is as follows.

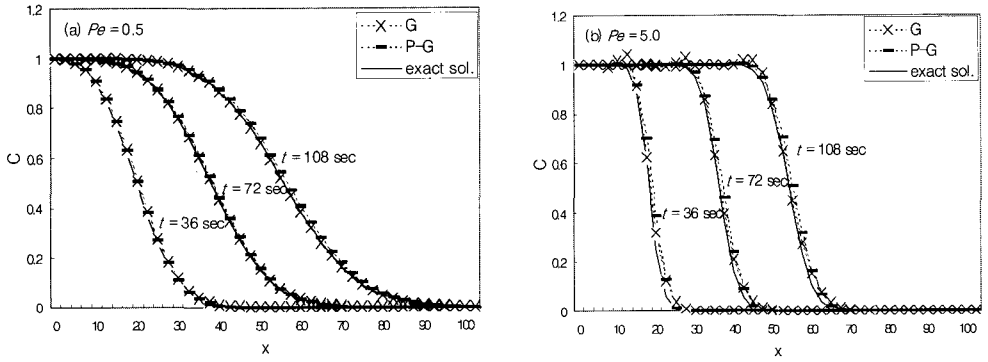

Fig. 1 Result of continuous injection from the transverse line source

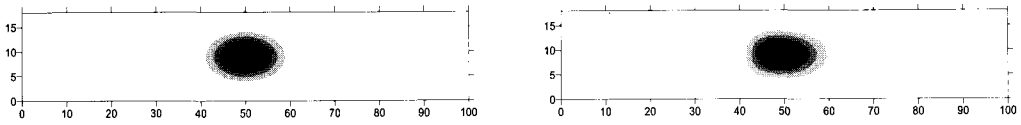

(a) analytical (b) numerical

Fig. 2 Contour of the results of instantaneous injection from the point source

$$C = \frac{M}{4\pi t\sqrt{D_x D_y}} \exp\left[-\frac{(x-Ut)^2}{4D_x t}\right] \sum_{n=-\infty}^{\infty} \exp\left[-\frac{(y+nw)^2}{4D_y t}\right] \tag{14}$$

where M is the injected mass, n is the number of reflection at the both sides of the channel, and w is the channel width. Fig. (2) shows the result of this comparison in the contour form. All the conditions of this simulation are same as that of the line source problem except for the $D_x = 0.1 \ m^2/\sec$, $D_y = 0.03 \ m^2/\sec$. Each

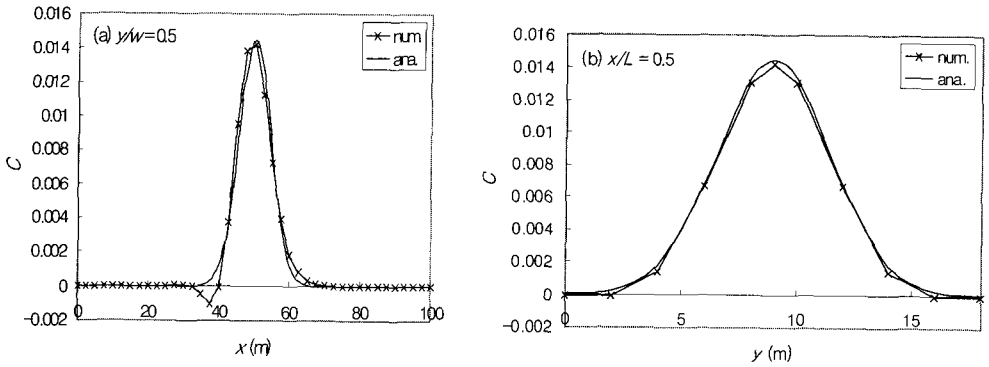

Fig. 3 Results of instantaneous injection from the point source

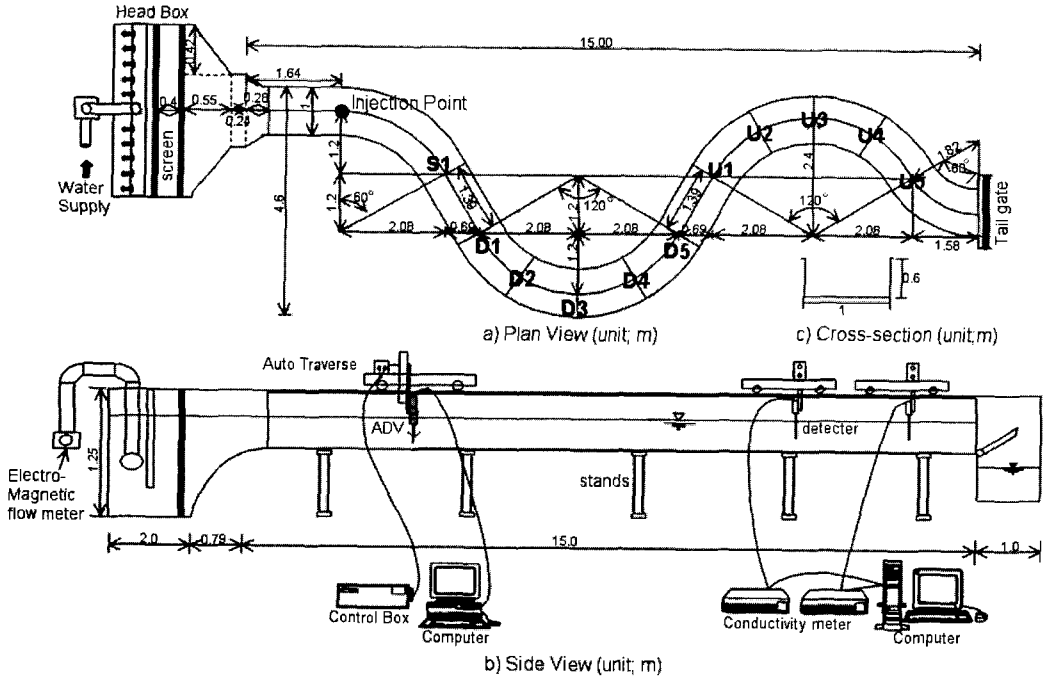

Fig. 4 Experimental S-curved channel

contour shows little difference in the shape of the concentration distribution. For more precise comparison, the concentration curve in the x-direction coinciding with the centerline of the channel and that of the y-direction at the centered cross section were plotted in the Fig. (3). These graph shows that the numerical model produces very similar result with the analytical solution.

4. APPLICATION TO THE S-CURVED CHANNEL

4.1 Experimental Data

The S-curved laboratory channel was constructed to conduct experiment as depicted in Fig. (4). To realize the meander pattern of natural streams, the channel was designed with reference to previous studies such as Leopold and Wolman (1960), Chang (1971), Krishnappan and Lau (1977), Holly (1985) and Guymer (1998). The considered hydraulic factors were channel width, radius of curvature, central angle, wavelength, and so on. This S-curved laboratory channel was 15 m long, 1 m wide, and 0.6 m deep. It consists of circular arcs connected by straight sections. The radius of curvature is 2.4m, the wavelength is 9.7m, and the central angle is 120. The cross-section of the channel is rectangular.

An electromagnetic flowmeter was installed in the water supply pipe to continuously measure the discharge passing through the channel. A point gauge was used to measure the flow depth. A micro-ADV, developed by Son-Tek, was used to measure the three-dimensional components of velocity and turbulence. The micro-ADV operates on a pulse-to-pulse coherent Doppler shift to provide a three-component velocity at a rate of 50 Hz. Especially, in this study, the side-looking ADV was used to measure whole region of cross-section. The measuring sections are presented in the Fig. (4a) as S1, D1, D2,··· etc. and in each section there are 15 points for velocity measurements.

The concentration measurements were made with the electrode conductivity meter, which was developed by KENEK. Six electrode conductivity meter probes were arranged at a transection. The probe calibration for the response to concentration was performed by a series of standard salt solutions whose range were from 0 ppm to 10,000 ppm.

The several cases of experiments were conducted for mixing in the meandering channel

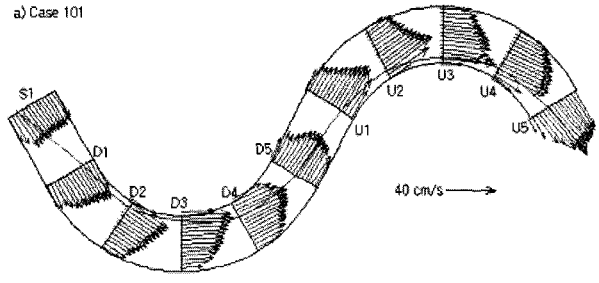

Fig. 5 Experimental result of the velocity field of case 101

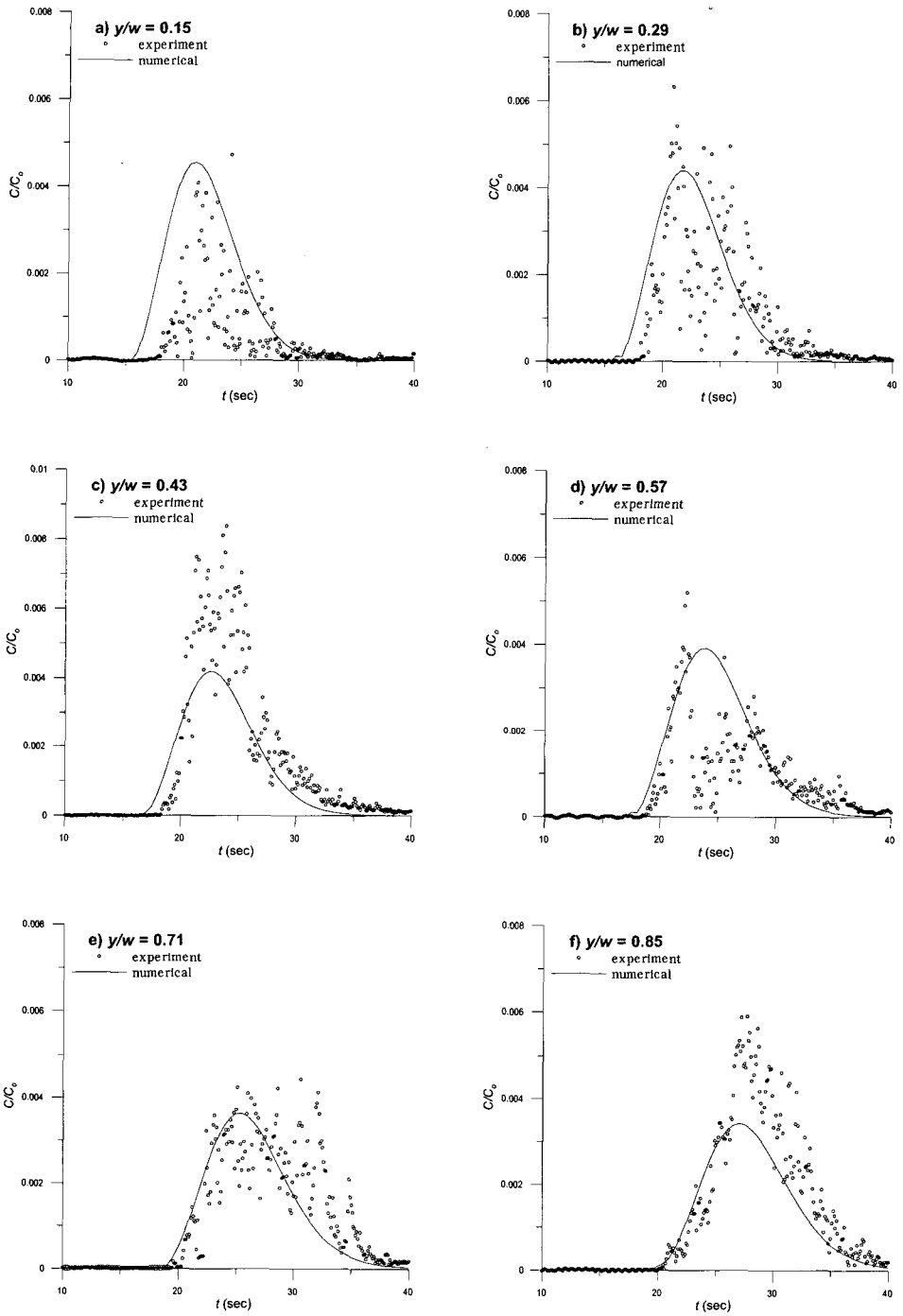

Fig. 6 Relative concentration vs. time graph of experimental data and numerical result for measuring section D3

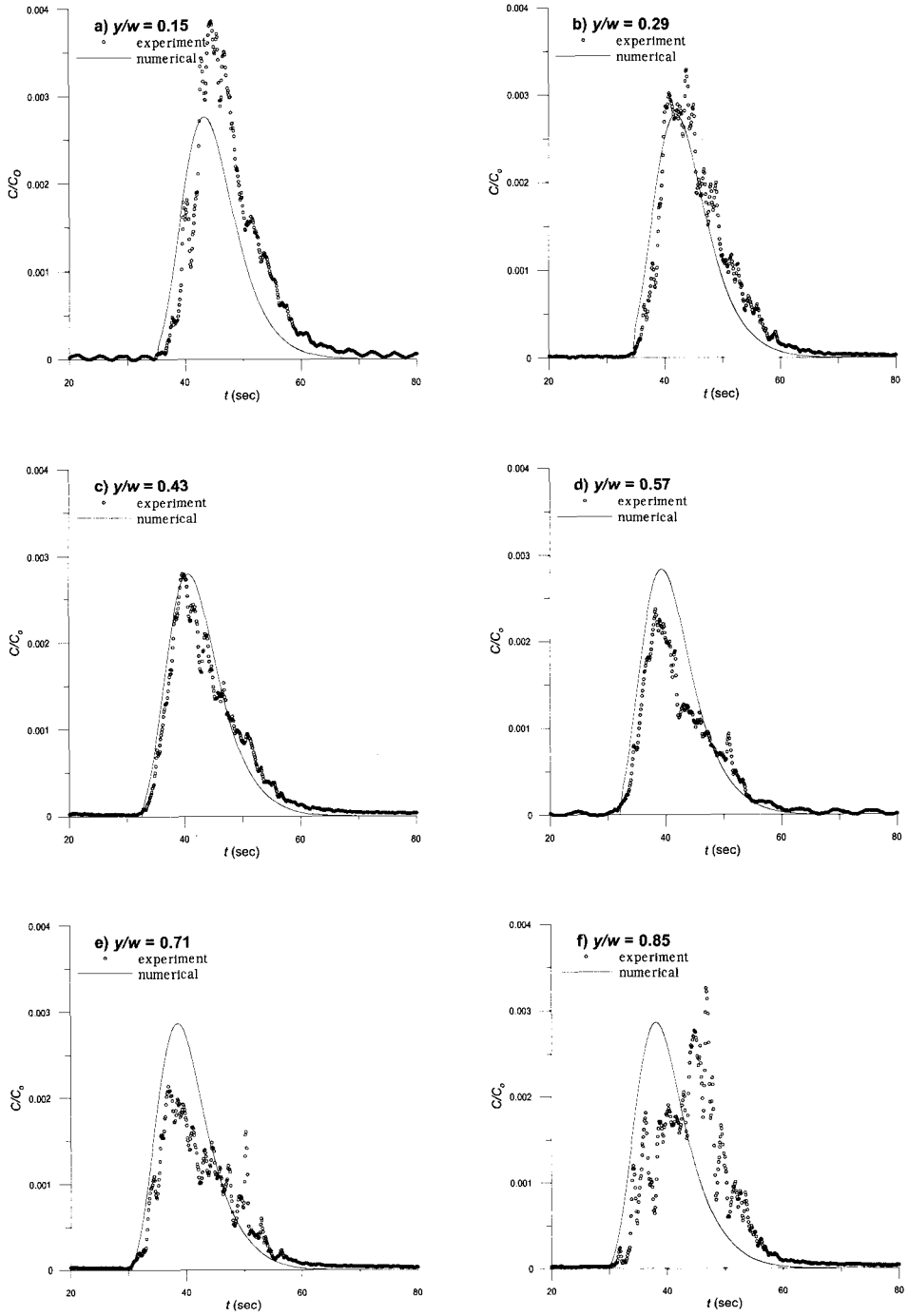

Fig. 7 Relative concentration vs. time graph of experimental data and numerical result for measuring section U3

under various conditions of the flowrate and water depth. At first the flow velocity field was measured in 11 sections. The input data of the velocity field for the numerical model were linearly interpolated for each element of meandering channel. The measured data of flow velocity for typical case is depicted in Fig. (5). In this figure, depth averaged velocities were obtained by averaging velocity data at two vertical points and the curved line in the channel denotes the line of maximum velocity. The noticeable phenomenon is that the maximum velocity occurs taking the shortest course along the channel, irrespective of flow conditions. In natural stream, however, it has been known that the maximum velocity occurred along the line which appeared near the outer bank.

As the tracer of the mixing experiments, 250,000 ppm salt solution was used. The injected point is the center of the section in which the S-meandering is beginning. The injection equipment has one hole of 1.5 cm diameter where the injected substance comes out. The measuring sections of the concentration are D1, D3, U1, U3. There are 6 measuring points for each cross-section.

4.2 Analysis of results

The relative concentration vs. time graph of experimental and numerical results at six measuring points for Sections D3 and U3 are presented in Fig.'s (6)-(7). In these figures, y denotes the distance from the left side of the channel, and w denotes the channel width. In the numerical simulation, D_x and D_y were selected so the best-fit value to the experimental data by trial and error with initial values from Eq. (15). The values of D_x and D_y are fitted as 0.01 $m^2/\sec$ and 0.001 $m^2/\sec$, respectively.

$$D_x = 5.93 d_c u^*, \quad D_y = \beta d_c u^* \tag{15}$$

where u^* is shear velocity and constant β varies from 0.093 to 0.24.

In Section D3 as in the Fig. (6), the experimental data show some fluctuations, so it can be said that the vertical mixing is not stabilized until this section. As one can see in this figure, the advection of the experiment is well-depicted by the numerical model. But the difference of the peak values between these two results in each measuring point is considerably large at several lateral locations.

In Section U3, shown in the Fig. (7) the experimental results are stabilized almost completely and the experimental and numerical results are matched well. Both the values and its positions of peak concentrations of the measured data are well simulated by the numerical model.

In the Fig. (8), the peak concentration C_p, time to peak t_p, the average of time $\bar{t}$, and the variance of time σ^2 for Sections D1, D3, U1, U3 were compared. The peak concentration isn't estimated well by the numerical simulation especially for the nearer sections from the injection point as shown in the Fig. (8a). However, the time to peak concentration matched well as shown in the Fig. (8b). In the Fig. (8c), the numerical simulation slightly underestimate the experimental result with respect to the average value of time. However, as shown in Fig. (8d), the variances of the numerical results are significantly smaller than those of experimental results. Variances of experimental data increases rapidly as the injected substance arrived at the section U1 and U3 while that of numerical results increases a little bit relatively.

For further application, the continuous point source injection in the experimental S-curved channel was simulated and compared with the

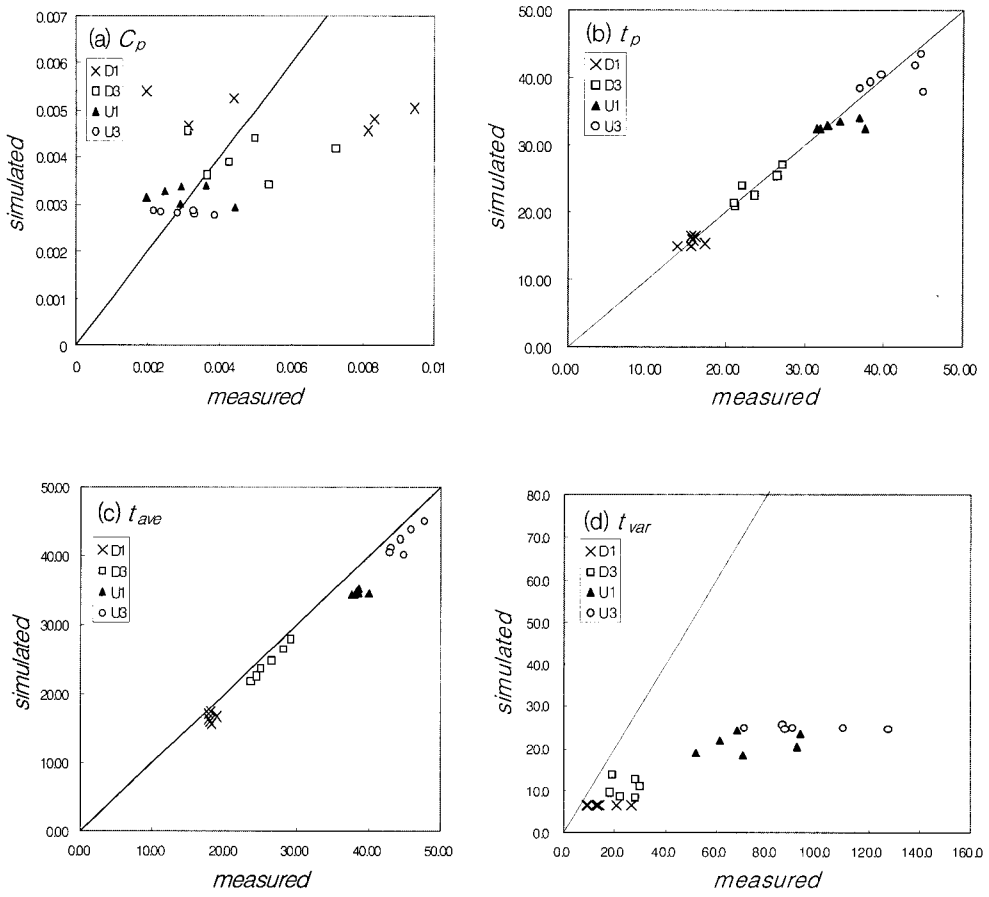

Fig. 8 Comparison about the several characteristics of the concentration distribution with respect to time

result by RMA4 (Environmental Modeling Research Lab., 2000). The continuous injection condition is difficult to be conducted at the experiment because it needs the large tank for the tracer. The simulation results by the numerical model and RMA4 are depicted in Fig. (9). These simulations have some different condition. The numerical model uses SUPG method for the formulation but the RMA4 uses standard Galerkin method. In the Fig. (9), the solution by the numerical model in this study has more dispersion effect produced by artificial diffusion which smooth the oscillating solution. Because of this smoothing effect, the mesh size of the numerical model doesn't have to be so fine as RMA4 requires.

Dispersion coefficients D_x and D_y are fixed in both RMA4 and the model of this study. However, in meandering channel such as the experimental channel used in this study, these coefficients are variable depending on the flow direction (Piasecki and Katopodes, 1999). More experimental works and the modification of governing equation are needed to account for

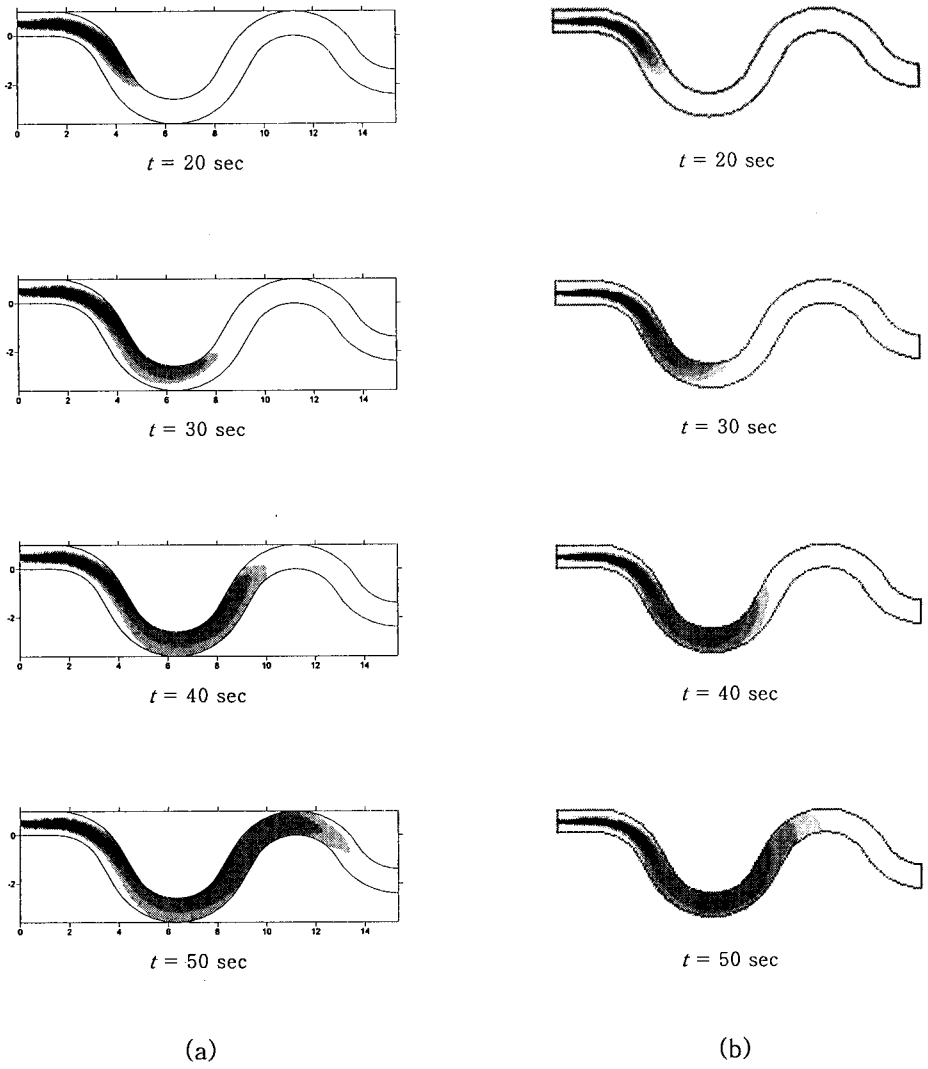

Fig. 9 The contour of the simulation result with the continuous injection; (a) Numerical result (b) Result by RMA4

the variability of dispersion coefficients.

5. CONCLUSION

Two-dimensional dispersion was modeled using the finite element method. Numerical simulations were tested against the analytical solutions for straight channels. Experiments were conducted to verify the performance of the numerical model in the curved channel.

In the transverse line source example in the straight channel, the numerical solution by standard Galerkin method makes a wiggling solution as the Peclet number become large. This result shows that the standard Galerkin method is not only inappropriate for steady-state problems, which is well-known, but also for the

transient problems. Thus, it is concluded that also in the transient problem there is difficulty in simulation by standard Galerkin method.

Although the upwind Petrov-Galerkin method didn't show the critical dependence of the Galerkin method on the Peclet number, it still gave more accurate solutions when the Peclet number is small. This can be interpreted as the effect of the artificial diffusion by the upwind formulation is large for the comparatively small diffusion. So in this two-dimensional transient problem, the optimal damping factor adapted from the one-dimensional case doesn't give such an accuracy as the one-dimensional steady-state problem.

Now that all these test applications above show the applicability of the numerical model constructed in this study, the real experimental concentration data could be compared with the simulation results by the numerical model. In this comparison, the experimental data of the initial mixing in the near-field is so unstable that the numerical result could not be fitted well. But once the experimental mixing become stable in the mid-field zone, the numerical results and the experimental results matched well each other. Therefore, it can be concluded that this numerical model can be applied to the real two-dimensional mixing process.

The SUPG method was used to the formulation which is different from the commercial simulation software RMA4 that used standard Galerkin method. With the proposed numerical model, the oscillation effect in the solution which is occurring when we used standard Galerkin method was smoothed, so the mesh size doesn't have to be so small as the RMA4 requires. That gives the reduction of the time for simulation.

6. ACKNOWLEDGEMENT

This research work was supported by the 21C Frontier project of the Ministry of the Science and Technology. This research work has been conducted in the Research Institute of Engineering Science of Seoul National University, Seoul, Korea. The authors are grateful to Kyoung Oh Back and Ki Hoon Sung for their help in the laboratory experiments.

REFERENCES

Barret, K.E. (1974). "The numerical solution of singular perturbation boundary value problem." *J. Mech. and Appl. Math.*, 27, 57-68.

Basha, H.A. (1997). "Analytical model of two-dimensional dispersion in laterally nonuniform axial velocity distributions." *J. Hydr. Engrg.*, 123, 853-862.

Brooks, A.N., and Hughes, T.J.R. (1982). "Streamline upwind/ Petrov-Galerkin formulation for convection dominated flows with particular emphasis on the incompressible Navier Stokes equation." *Comp. Meth. Appl. Mech. Engrg.*, 32, 199-259.

Chang, Y. (1971). Lateral mixing in meandering channels. Ph.D. Thesis, Univ. of Iowa City, Iowa.

Christie, I., Griffiths, D.F., Mitchell, A.R., and Zienkiewicz, O.C. (1976). "Finite element methods for second order differential equations with significant first derivatives." Int. *J. Num. Meth. Engrg.*, 10, 1389-1396.

Guymer, I. (1998). "Longitudinal dispersion in sinuous channel with change in shape." *J. Hydr. Engrg.*, 124, 33-40.

Heinrich, J.C., Huyakorn, P.S., Zienkiewicz, O.C., and Mitchell, A.R. (1977). " An upwind finite element scheme for two dimensional equation with significant first derivatives."

Int. J. Num. Meth. Engrg., 11, 131-144.

Han, K.Y. and Kim, S.H. (2000). " Advection-Diffusion Analysis in a River by Petrov-Galerkin Method." *J. KSCE*, 20, 251-259 (In Korean).

Holly, F.M., Jr. (1985). " Two-dimensional mass dispersion in rivers." *Hydrology Paper* No. 78, Colorado State Univ., Fort Collins, Colorado.

Kim. H.I., Lee, J.S., Heo, J.H., Cho, W.C. (1998). " A Study on the Contaminant Transport Characteristics in Han River." *J. KWRA*, 31, 85-93 (In Korean).

Kim, S.H. and Han, K.Y. (2000). " 2-D Water Quality Analysis in Nakdong River by Finite Element Method." *J. KSCE*, 20, 525-533 (In Korean).

Krishnappan, B.G., and Lau, Y.L. (1977). " Transverse mixing in meandering channels with varying bottom topography." *J. Hydr. Res.*, 15, 351-371.

Leopold, L.B., and Wolman, M.G. (1960). " Modeling transverse mixing in natural stream." *J. Hydr. Div.*, 107, 209-226.

Piasecki, M. and Katopodes, N.D. (1999). " Identification of Stream Dispersion Coefficients by Adjoint Sensitivity Method." *J. Hydr. Engrg.*, 125, 714-724.

Runchall, A.K., and Wolfstein, M. (1969). " Numerical integration procedure for the steady state Navier-Stokes equations." *J. Mech. Engrg. Sci.*, 11, 445-453.

Spalding, D.B. (1972). " A novel finite difference formulation for differential equation involving both first and second derivatives." *Int. J. Num. Meth. Engrg.*, 4, 551-559.

Zienkiewicz, O.C., Gallagher, R.H., and Hood, P. (1976). Newtonian and non-Newtonian viscous incompressible flow. Temperature induced flows and finite element solution, in *The mathematics of finite elements and applications* (ed. Whiteman, J.), Vol. II, Academic Press, London.

Zienkiewicz, O.C., and Taylor, R.L. (2000). *The finite element method, Vol. 3*, 5th Ed., Butterworth-Heinemann, Oxford.

Environmental Modeling Research Lab. (2000). SMS Surface water modeling system, tutorial, version 7.0, Brigham Young University.

Graduate Student, Dept. of Civil Engineering, Seoul National University, Seoul, Korea. (E-mail: lmeun88@snu.ac.kr)

Post Doctor, Dept. of Civil Engineering, Seoul National University, Seoul, Korea. (E-mail: yhkim98@gong.snu.ac.kr)

Professor, Dept. of Civil Engineering, Seoul National University, Seoul, Korea. (E-mail: seoilwon@plaza.snu.ac.kr)